Contribution from the Department of Chemistry,
University of Houston, Houston, Texas 77004

Electrochemical Studies of a Novel Ruthenium(II, III) Dimer, $Ru_2(HNOCCF_3)_4Cl$

T. MALINSKI, D. CHANG, F. N. FELDMANN, J. L. BEAR,* and K. M. KADISH*

Received April 15, 1983

The electrochemical reduction of a novel ruthenium($II^1/_2$) dimer, $Ru_2(HNOCCF_3)_4Cl$, was investigated in 11 nonaqueous solvents containing either TBAP or (TBA)Cl as supporting electrolyte. In DMA, DMF, Me_2SO, and CH_3OH, or in less strongly complexing solvents containing excess Cl^-, only a single one-electron-transfer process was observed. In contrast, reduction in all other solvents gave rise to current–voltage curves with either three or four peaks. The products of each electron-transfer reaction were investigated by spectroelectrochemical techniques and showed evidence for formation of Ru(II) dimers as well as further reduced complexes of $Ru_2(HNOCCF_3)_4$. Finally, comparisons were made between the overall reduction mechanism of the novel amidato complex and that of the carboxylato complex $Ru_2(O_2CC_3H_7)_4Cl$.

Introduction

Dinuclear rhodium and ruthenium complexes are unique among the strongly metal–metal-bonded complexes because of the sensitivity of their orbital patterns with respect to axial and equatorial ligand perturbations. We have carried out electrochemical studies on dinuclear rhodium tetracarboxylates and have shown that the HOMO and LUMO are lowered in energy substantially by electron-withdrawing substituents on the carboxylate ion.[1] From these studies it became apparent that in order to lower the oxidation potential for the formation of the radical cation, bridging ligands other than carboxylates would have to be found. Recently we have shown that amidato bridging ions, which can be altered by substituents at both the amide carbon and nitrogen atoms, allow us to "tune" the orbital energies of the rhodium dimer over a much wider range.[2,3] In fact, with the *N*-phenylacetamidato-bridged dirhodium complex we observe a second reversible oxidation to an apparent dirhodium(III) species.[3]

Unlike the dinuclear rhodium complexes, the most stable form of diruthenium tetracarboxylates contains the metal atoms in formally different oxidation states. The dimeric complex is paramagnetic with three unpaired electrons. Investigations of these dinuclear ruthenium complexes have included methods of preparation,[4-9] standard characterization,[10-16] and magnetic properties.[4,5,16,17] It was found that the average Ru oxidation state per nuclear unit is nonintegral and is probably close to +2.5.[8,10] Some electrochemical properties of one representative member of these series, $Ru_2(O_2CC_3H_7)_4Cl$, have been determined.[17]

In spite of many attempts, crystalline samples of $Ru_2(O_2CR)_4$ have never been obtained, although the species has been postulated to exist in solution.[8,10,17] It was formerly believed that the phosphine adduct of the unknown tetrakis(acetato)diruthenium(II) had been obtained,[8] but this was later proven to be $Ru_3O(CO_2Me)_6(PPh_3)_3$.[6]

In the present paper we report the synthesis, physical properties, and electrochemistry of a new diruthenium($II^1/_2$) complex which is similar to $Ru_2(O_2CR)_4X$ but which has trifluoroacetamidato (CF_3CONH) in place of carboxylato bridging ligands. This compound (shown in Figure 1b) provides a new example of a Ru($II^1/_2$) dimer, which is stable and can be altered chemically by substitution on the amide carbon and nitrogen atoms. This complex also provides new possibilities for studying the influence of a bridging ligand on the reactivity of a diruthenium center.

Experimental Section

Synthesis of $Ru_2(HNOCCF_3)_4Cl$. $Ru_2(HNOCCF_3)_4Cl$ was synthesized by the reaction of trifluoroacetamide (CF_3CONH_2) with $Ru_2(O_2CCH_3)_4Cl$. $Ru_2(O_2CCH_3)_4Cl$ was prepared with use of a procedure previously described.[5] A 25-g quantity of CF_3CONH_2 was combined with 0.5 g of $Ru_2(O_2CCH_3)_4Cl$ under nitrogen. This mixture was then heated to 127 °C and stirred for 60 h. Following sublimation of excess CF_3CONH_2, the entire procedure was repeated with 25 g of fresh CF_3CONH_2 to ensure complete exchange. Excess CF_3CONH_2 was then removed by sublimation. The crude product was recrystallized three times from a mixture of methanol and toluene and dried under vacuum.

Anal. Calcd for $Ru_2(HNOCCF_3)_4Cl$: C, 14.01; H, 0.59; N, 8.17; Cl, 5.17. Found: C, 14.19; H, 0.68; N, 8.08; Cl, 5.31. IR (Nujol mull): 730, 855, 1160, 1260, 1580, 3380 cm^{-1}. Magnetic moment per Ru atom (Me_2SO): 2.86 μ_B at 294 K (Evans method); 2.87 μ_B (solid) at 297 K. ESR: $g_\parallel = 2.060$; $g_\perp = 4.119$.

Reagents and Instrumentation. Methylene chloride, CH_2Cl_2, obtained from Fisher Scientific Co. as technical grade, was twice distilled from P_2O_5 and stored in the dark over activated 4-Å molecular sieves. Dimethylformamide, DMF, obtained from Eastman Chemicals, was first shaken with KOH, then distilled from CaO under N_2, and stored over 4-Å molecular sieves before use. Dichloroethane, $EtCl_2$ (Matheson Coleman and Bell), acetonitrile, CH_3CN (Matheson Coleman and Bell), acetone, $(CH_3)_2CO$ (Matheson Coleman and Bell), dimethylacetamide, DMA (Fisher Scientific), dimethyl sulfoxide, Me_2SO (Eastman Chemical), *n*-butyronitrile, *n*-PrCN (Aldrich), nitromethane, CH_3NO_2 (Aldrich), methanol, CH_3OH (Baker), and tetrahydrofuran, THF (Matheson Coleman and Bell), were all received as reagent grade from the manufacturer and were dried over 4-Å molecular sieves prior to use. For all electrochemical experiments, the solvents contained 0.1 M supporting electrolyte. The following were utilized as supporting electrolytes: tetrabutylammonium perchlorate (TBAP), tetramethylammonium chloride ((TMA)Cl), and tetrabutylammonium chloride ((TBA)Cl). All of these were recrystallized and dried in vacuo prior to use.

Cyclic voltammetric measurements were made by using the conventional three-electrode configuration and an IBM Model EC 225 voltammetric analyzer. A platinum button served as a working

(1) Das, K.; Kadish, K. M.; Bear, J. L. *Inorg. Chem.* **1978**, *17* (4), 930.
(2) Kadish, K. M.; Lançon, D.; Dennis, A. M.; Bear, J. L. *Inorg. Chem.* **1982**, *21* (8), 2987.
(3) Duncan, J.; Malinski, T.; Zhu, T. P.; Hu, Z. S.; Kadish, K. M.; Bear, J. L. *J. Am. Chem. Soc.* **1982**, *104*, 5507.
(4) Makaida, M.; Nomura, T.; Ishimori, T. *Bull. Chem. Soc. Jpn.* **1972**, *45*, 2143.
(5) Stephenson, T. A.; Wilkinson, G. *J. Inorg. Nucl. Chem.* **1966**, *28*, 2285.
(6) Cotton, F. A.; Norman, J. G., Jr. *Inorg. Chim. Acta* **1972**, *6*, 411.
(7) Mukaida, M.; Nomura, T.; Ishimori, T. *Bull. Chem. Soc. Jpn.* **1967**, *40*, 2462.
(8) Legzdins, P.; Mitchell, R. W.; Rempel, G. L.; Ruddick, J. D.; Wilkinson, G. *J. Chem. Soc. A* **1970**, 3322.
(9) Mitchell, R. W.; Spencer, A.; Wilkinson, G. *J. Chem. Soc., Dalton Trans.* **1973**, 846.
(10) Bennett, M. J.; Caulton, K. G.; Cotton, F. A. *Inorg. Chem.* **1969**, *8*, 1.
(11) Bino, A.; Cotton, F. A.; Felthouse, T. *Inorg. Chem.* **1979**, *18* (9), 2599.
(12) Clark, R. J. H.; Franks, M. L. *J. Chem. Soc., Dalton Trans.* **1976**, 1825.
(13) Norman, J. G., Jr.; Kolari, H. J. *J. Am. Chem. Soc.* **1978**, *100*, 791.
(14) Warren, L. F.; Goedken, U. L. *J. Chem. Soc., Chem. Commun.* **1978**, 909.
(15) Wilson, C. R.; Taube, H. *Inorg. Chem.* **1975**, *14*, 2276.
(16) Norman, J. G., Jr.; Renzoni, G. E.; Case, D. A. *J. Am. Chem. Soc.* **1979**, *101*, 5256.
(17) Cotton, F. A.; Pedersen, E. *Inorg. Chem.* **1975**, *14*, 388.

0020-1669/83/1322-3225$01.50/0

Table I. Peak Separations and Half-Wave Potentials for the Reduction of $Ru_2(HNOCCF_3)_4Cl$ in Nonaqueous Solvents[a]

solvent	supporting electrolyte	RED(1) $E_{p,a} - E_{p,c}$, mV	RED(1) $E_{1/2}$, V	RED(2) $E_{p,a} - E_{p,c}$, mV	RED(2) $E_{1/2}$, V	RED(3) $E_{p,a} - E_{p,c}$, mV	RED(3) $E_{1/2}$, V	RED(4) $E_{p,c}$, V
$EtCl_2$	0.1 M TBAP			210	−0.02	110	−0.32	(−1.44)[b]
CH_2Cl_2	0.1 M TBAP			200	−0.03	100	−0.33	(−1.44)[b]
$(CH_3)_2CO$	0.1 M TBAP			240	−0.09	160	−0.37	[c]
CH_3NO_2	0.1 M TBAP			170	−0.05	140	−0.33	[c]
CH_3CN	0.1 M TBAP	80	(0.00)[d]	120	−0.06	140	−0.30	(−1.41)[b]
	0.1 M (TBA)Cl					90	−0.34	
	0.02 M (TMA)Cl					120	−0.34	
n-PrCN	0.1 M TBAP	100	0.01	200	−0.04	150	−0.30	(−1.40)[b]
THF	0.1 M TBAP	140	0.01	200	−0.07	170	−0.35	(−1.31)[b]
DMF	0.1 M TBAP	210	−0.22					
DMA	0.1 M TBAP	210	−0.22					
Me_2SO	0.1 M TBAP	100	−0.19					
	0.1 M (TBA)Cl					170	−0.34	
	0.02 M (TMA)Cl					130	−0.34	
CH_3OH	0.1 M TBAP	60	−0.07					

[a] Scan rate 100 mV/s. [b] Irreversible reaction. [c] Not observed because of solvent limit. [d] Potential reported as $E_{p,c}$.

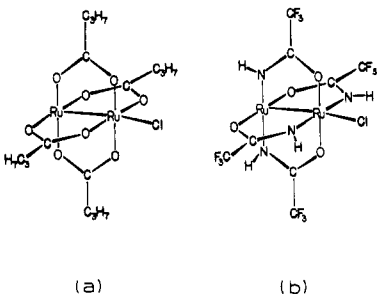

Figure 1. Structure of (a) $Ru_2(O_2CC_3H_7)_4Cl$ and (b) $Ru_2(HNOCCF_3)_4Cl$.

electrode and the platinum wire as a counterelectrode for conventional cyclic voltammetric measurements. A saturated calomel electrode (SCE), separated from the bulk of the solution by a fritted glass disk, was used as the reference electrode. Current–voltage curves were collected on a Houston Instruments Omnigraphic X-Y recorder at scan rates from 0.05 to 0.30 V/s and on a Tektronix 5111 storage oscilloscope using a Tektronix C-5A oscilloscope camera at scan rates from 0.5 to 10 V/s. For controlled-potential coulometry and controlled-potential electrolysis, a Princeton Applied Research Model 173 potentiostat was used to control the potential. Integration of the current–time curve was achieved by means of a PAR Model 179 integrator. A three-electrode configuration was used, consisting of a Pt-wire mesh working electrode, a Pt-wire counterelectrode separated from the main solution by a glass frit, and an SCE as the reference electrode. The coulometric cell contained a quartz window at the bottom, allowing the electronic spectra of the reactant and product to be taken in situ.

Deaeration and stirring were achieved by means of a stream of high-purity nitrogen, which was passed throughout the solution. Spectroelectrochemistry was performed in a bulk cell, which followed the design of Fajer et al[18] and had an optical path length of 0.19 cm. This spectroelectrochemical cell was coupled with a Tracor Northern 1710 optical spectrometer/multichannel analyzer to obtain time-resolved spectra. The spectra result from the signal averaging of 100 5-ms spectral acquisitions. Each acquisition represents a single spectrum from 325 to 950 nm, simultaneously recorded by a double-array detector with a resolution of 1.2 nm/channel.

ESR spectra at 77 K were recorded on an IBM Model ER 100D spectrometer, equipped with an ER 040-X microwave bridge and an ER 080 power supply. The cavity was cooled by a stream of liquid nitrogen that was constantly passed through the variable-temperature insert. The samples were introduced into the cavity in a sealed quartz tube immersed in a liquid-nitrogen Dewar. The g values were measured relative to diphenylpicrylhydrazyl (DPPH) (g = 2.0036 ± 0.0003).

(18) Fajer, J.; Borg, D. C.; Forman, A.; Dolphin, D.; Felton, R. H. *J. Am. Chem. Soc.* **1970**, *92*, 3451.

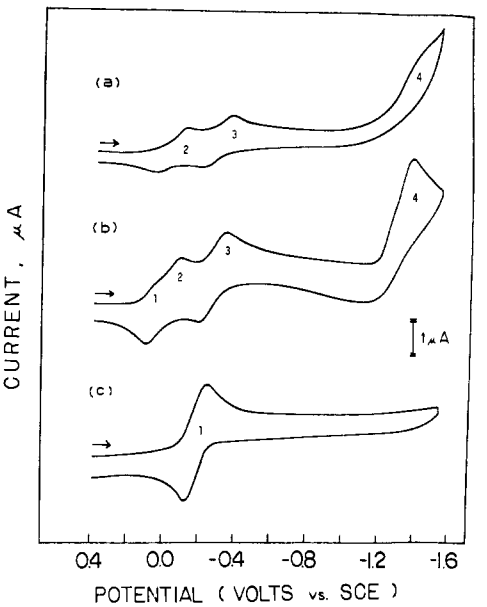

Figure 2. Cyclic voltammograms of $Ru_2(HNOCCF_3)_4Cl$ in (a) CH_2Cl_2 (0.1 M TBAP), (b) CH_3CN (0.1 M TBAP), and (c) Me_2SO (0.1 M TBAP). Scan rate = 0.1 V/s.

Magnetic moment measurements were done both in solution and in the solid state. A Princeton Applied Research Model 155 vibrating-sample magnetometer and Varian Model T-60 NMR spectrometer were utilized for the solid state and solution state, respectively. Infrared spectra were taken in Nujol and hexachlorobutadiene mulls with a Beckman 4250 spectrometer.

Results and Discussion

Electrochemical Properties of $Ru_2(HNOCCF_3)_4Cl$. Depending upon the solvent and the supporting electrolyte (TBAP, (TBA)Cl, or (TMA)Cl), a number of different current–voltage curves were obtained for the reduction of $Ru_2(HNOCCF_3)_4Cl$. In nonbonding solvents containing TBAP, three redox processes were observed in the range of potential between +1.8 and −1.8 V. In solvents such as CH_3CN and THF, four processes were observed. No oxidations were observed, and only reductions occurred. The first reduction was found at $\simeq$0.00 V, the second at $\lesssim$−0.06 V, and the third at $\lesssim$−0.3 V, while the fourth reduction was at $\simeq$−1.41 V and had a peak current about the same as the sum of peak currents for three processes occurring between 0.00 and −0.5 V. In strongly bonding solvents such as Me_2SO, DMA, DMF, or CH_3OH only a single process was observed. This occurred between 0.0 V and −0.3 V, depending on the solvent.

Table II. Stepwise Coulometric Measurements for the Controlled-Potential Reduction of $Ru_2(HNOCCF_3)_4Cl$ in CH_2Cl_2, CH_3CN, and Me_2SO Solution[a]

solvent	supporting electrolyte	e consumed, faraday			
		wave 1	wave 2	wave 3	wave 4
CH_2Cl_2	0.1 M TBAP	*c*	0.49 ± 0.02	0.50 ± 0.02	0.95 ± 0.05
	0.1 M (TBA)Cl	*c*	*c*	0.99 ± 0.02	*c*
CH_3CN	0.1 M TBAP		0.48 ± 0.03[b]	0.51 ± 0.02	1.04 ± 0.06
	0.1 M (TBA)Cl	*c*	*c*	0.97 ± 0.02	*c*
	0.02 M (TMA)Cl	*c*	*c*	0.98 ± 0.04	*c*
Me_2SO	0.1 M TBAP	0.95 ± 0.06	*c*	*c*	*c*
	0.02 M (TMA)Cl	0.99 ± 0.03	*c*	*c*	*c*

[a] All values represent the average of three measurements with the deviations given as standard deviations from the mean. [b] Value also includes small contribution from wave 1. [c] No reaction.

The reduction of $Ru_2(HNOCCF_3)_4Cl$ was investigated in 11 nonaqueous solvents. Figure 2 illustrates typical cyclic voltammograms obtained in three of these solvents (CH_2Cl_2, CH_3CN, and Me_2SO) with 0.1 M TBAP as supporting electrolyte, and a summary of half-wave potentials and peak separations with different supporting electrolytes is given in Table I. As seen in Figure 2a, two well-defined quasi-reversible waves and one irreversible wave are observed in CH_2Cl_2. The first wave has $E_{1/2} = -0.03$ V, the second $E_{1/2} = -0.33$ V, and the third, which is totally irreversible, $E_{p,c} \simeq -1.44$ V. The potential separations $E_p - E_{p/2}$ and $E_{p,a} - E_{p,c}$ at low scan rates for the first two reductions range between 70 and 100 mV and are in the range predicted for quasi-reversible, one-electron transfer. The peak current for both reversible processes is proportional to the square root of scan rate and $i_{p,a}/i_{p,c} \simeq 1$. The peak current of wave 3 is approximately equal to the sum of peak currents of waves 1 and 2.

In CH_3CN containing 0.1 M TBAP (Figure 2b), four reduction peaks are observed. Half-wave potentials for the second and third reductions are −0.06 and −0.30 V, while $E_{p,c}$ for the fourth reduction is −1.41 V. As seen in Table I, all three values are similar to those measured in CH_2Cl_2. The first wave observed for reduction of $Ru_2(HNOCCF_3)_4Cl$ in CH_3CN (at $E_{p,c} = 0.00$ V) has the shape of one-electron quasi-reversible reduction, but unlike a "normal" diffusion-controlled process, the current for this reduction significantly decreases with increasing concentration of TBAP. At the same time, the currents for wave 2 increase with [TBAP]. The currents for wave 3 are independent of TBAP concentration. Wave 4 has the shape of an irreversible electron transfer, and the currents for this process are also independent of TBAP concentration. This is evident in Figure 2b and indicates that two electrochemical processes having similar half-wave potentials probably occur, with the total peak current of wave 4 being a sum of these two processes. At all TBAP concentrations between 0.1 and 0.8 M the peak current of wave 4 is approximately equal to the sum of the peak currents for waves 1, 2, and 3. At a potential of about −1.35 V, an inflection on wave 4 is observed. Finally in Me_2SO, 0.1 M TBAP, only one quasi-reversible, single-electron-transfer redox couple is observed at $E_{1/2} = -0.19$ V. This is shown in Figure 2c.

$Ru_2(HNOCCF_3)_4Cl$ was reduced at a controlled potential in each solvent, and the cyclic voltammograms were recorded before and after total electrolysis. Values of the faradays added during controlled-potential reduction of each solution in Figure 2 are shown in Table II. Controlled-potential reduction in CH_2Cl_2, first at a potential of −0.2 V and then at −0.6 V, showed that 0.49 and 0.50 faraday were transferred during the first and second reductions, respectively. Further stepping of the potential to −1.55 V gave 0.95 faraday for the wave at negative potentials (labeled wave 4 in Table II). The total number of faradays obtained for the reduction at the first and second step in CH_3CN (electrolysis at the plateau of wave 2) was 0.48. Approximately the same 0.5 faraday was found for the third reduction in CH_3CN. In this case, the fourth reduction gave 1.04 faradays. Finally, a value of 0.95 faraday was found for the single reduction observed in Me_2SO (wave 1, Figure 2).

The above coulometric data and voltammetric curves illustrated in Figure 2 suggest an equilibrium between different forms of axially complexed $Ru_2(HNOCCF_3)_4Cl$. In the solid state, $Ru_2(HNOCCF_3)_4Cl$ probably exists in a polymeric form with chloride ions bridging adjacent dinuclear ruthenium cations to form infinite zigzag chains of $(Ru–RuCl)_n$. Upon addition to solution, this polymeric structure is split to yield complexes of the form (S)Ru–RuCl or $[(S)Ru–Ru(S)]^+$ and $[ClRu–RuCl]^-$, where S is a solvent molecule. In the latter case, ion-pair formation can occur between the negatively and positively charged dimeric units.

In a nonbonding solvent such as CH_2Cl_2, the breaking up of the polymer is slow, but this increases significantly in the presence of chloride ions. After addition of (TBA)Cl to methylene chloride, the solubility of $Ru_2(HNOCCF_3)_4Cl$ increases from 10^{-5} M up to $\simeq 10^{-3}$ M. This is due to the reaction

$$[Ru–Ru(Cl)]_n + nCl^- \rightleftarrows n[ClRu–RuCl]^- \quad (1)$$

Breaking up of the polymer also occurs (although slowly) in the presence of ClO_4^-. In 0.1 M TBAP, CH_2Cl_2 solvent, two forms of ruthenium dimer with perchlorate and chloride ions as axial ligands can be envisioned. These are $[ClRu–RuCl]^-$ and $[ClO_4Ru–RuClO_4]^-$. In strongly bonding solvents, both Cl^- and ClO_4^- can be displaced by a solvent molecule, and only a single redox process occurs.

The single complex $[(S)Ru–Ru(S)]^+$ is present in strongly bonding solvents containing electrolyte, and only one reduction peak is observed. However, addition of excess Cl^- in the form of (TBA)Cl should shift the equilibrium from that of a bis-solvated species to that containing either one or two bound Cl^- ions. This is shown by eq 2 and 3, where S = Me_2SO.

$$[(Me_2SO)Ru–Ru(Me_2SO)]^+ + Cl^- \rightleftarrows ClRu–Ru(Me_2SO) + Me_2SO \quad (2)$$

$$ClRu–Ru(Me_2SO) + Cl^- \rightleftarrows [ClRu–RuCl]^- + Me_2SO \quad (3)$$

Reduction in the Presence of Excess Cl^-. In order to determine which, if any, of the reactants and products contained bound chloride ions, electrochemical reduction in CH_3CN and Me_2SO was investigated in the presence of excess Cl^- ions. This involved both electrochemical titrations of $Ru_2(HNOCCF_3)_4Cl$ in CH_3CN with Cl^- and a changing of the supporting electrolyte from 0.1 M TBAP to 0.1 M (TBA)Cl or (TMA)Cl.

The results of these experiments are shown in Figures 3 and 4. In the absence of Cl^- the current–voltage curve shown in Figure 3a is obtained. This curve, which has already been described, consists of three quasi-reversible reductions between 0.0 and −0.3 V and a single irreversible reduction at −1.41 V. Addition of Cl^- in the form of (TBA)Cl initially produced a

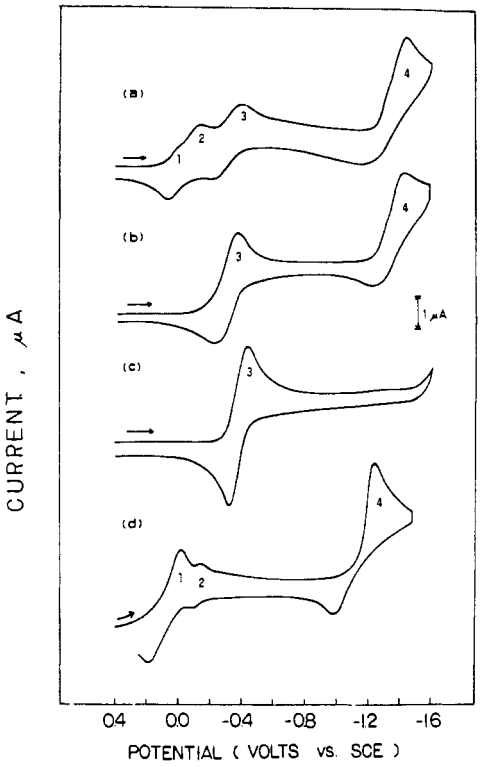

Figure 3. Cyclic voltammograms of $Ru_2(HNOCCF_3)_4Cl$ in CH_3CN, 0.1 M TBAP, at various ratios of $[Cl^-]/Ru_2(HNOCCF_3)_4Cl$: (a) 0/1; (b) 1/1; (c) 30/1. Part (d) is the cyclic voltammogram of $Ru_2(HNOCCF_3)_4Cl$ after addition of 1.0 equiv of Ag^+. Scan rate = 0.1 V/s.

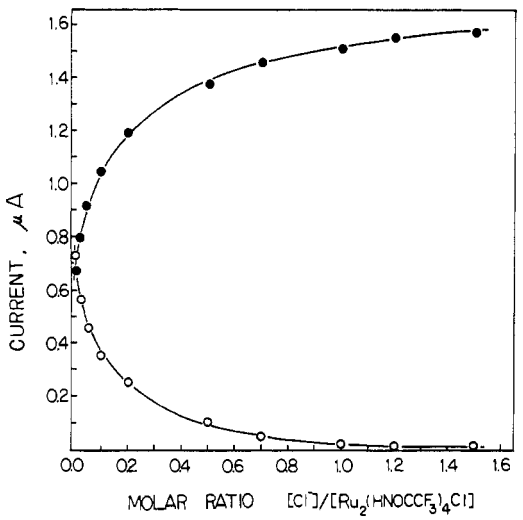

Figure 4. Dependence of peak currents for reduction processes 1–3 on the mole ratio $[Cl^-]/Ru_2(HNOCCF_3)_4Cl$ in CH_3CN, 0.1 M TBAP. The three reduction processes are identified in Figure 3. Currents are for the sum of peaks 1 + 2 (○) and for peak 3 (●).

decrease in the height of waves 1 and 2 with a concomitant increase in the height of wave 3. This is shown in Figure 4, which plots peak current for waves 1 + 2 and 3 as a function of the molar ratio $[Cl^-]/[Ru_2(HNOCCF_3)_4Cl]$. At a molar ratio of 1.0 the currents for waves 1 and 2 have dropped to zero and that of wave 3 has approximately doubled, as shown in Figure 3b. Under these conditions there was no apparent change in the currents for wave 4. Further additions of Cl^- resulted in a small increased current and a narrowing of the peak shape for wave 3 (which was originally at $E_{1/2} = -0.30$ V), suggesting an increased reversibility of the electrochemical process. This is shown in Figure 3c, which is illustrated at

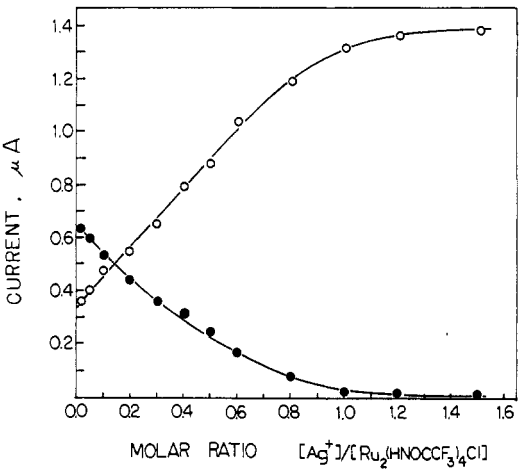

Figure 5. Dependence of peak currents for reduction processes 1–3 on the mole ratio $[Ag^+]/Ru_2(HNOCCF_3)_4Cl$ in CH_3CN, 0.1 M TBAP. The three reduction processes are identified in Figure 3. Currents are for peak 1 (○) and for peak 3 (●).

a $[Cl]^-/[Ru(HNOCCF_3)_4Cl]$ ratio of 30/1.

In addition to the changes in currents for waves 1, 2, and 3, increased Cl^- resulted in a negative shift of E_p for wave 4 such that, at a ratio of 30/1, the wave has been shifted beyond the potential range of the solvent. (The approximate cathodic shift of this wave is 120 mV/10-fold increase in Cl^- concentration.) Finally, in solutions containing 0.1 M (TBA)Cl a single reversible reduction is obtained. The potential for this reduction is −0.34 V and is listed in Table I for comparison with the other solutions.

The data in Figures 3 and 4 suggest that Cl^- is added to $Ru_2(HNOCCF_3)_4Cl$ to form the dichloro adduct $[Ru_2(HNOCCF_3)_4(Cl)_2]^-$. This suggestion was confirmed by spectral titrations (see discussion below), which show only a single Cl^- being added per dimeric unit. It is interesting to note from the electrochemical data that the potential for reduction of $[Ru_2(HNOCCF_3)_4Cl_2]^-$ is virtually identical with that for wave 3 in CH_3CN and might suggest that, in this solvent, this process is due to the same reacting species, namely the dichloro adduct, and the reduction can be written as shown in reaction 4.

$$[Ru_2(HNOCCF_3)_4Cl_2]^- + e^- \rightleftarrows [Ru_2(HNOCCF_3)_4Cl_2]^{2-} \quad (4)$$

Similar Cl^- titrations were carried out in Me_2SO. In this solvent a single wave is obtained at −0.19 V. During additions of Cl^- to $Ru_2(HNOCCF_3)_4Cl$ in Me_2SO only a single electron transfer reaction remained but a gradual cathodic shift of the wave was observed, until at high $[Cl^-]$ a constant value of $E_{1/2} = -0.34$ V was measured. This value, which is listed in Table I, is identical with that in CH_3CN and suggests formation of the dichloro $Ru(II^1/_2)$ complex in these solvents.

In order to confirm our hypothesis that a dichloro complex exists in CH_3CN, 0.1 M TBAP, titrations of this solution with $AgClO_4$ were performed and the potentials measured at various ratios of $[Ag^+]/[Ru_2(HNOCCF_3)_4Cl]$. This is shown in Figures 3d and 5. Stepwise additions of $AgClO_4$ resulted in a decrease of the currents for waves 2 and 3 and a concomitant increase in the currents for wave 1. This is shown in Figure 5. After addition of 1 equiv of Ag^+, wave 3 has completely dissappeared and only waves 1 and 2 remain. The sum of the currents of waves 1 and 2 is almost identical with that obtained for waves 1, 2, and 3. At the same time, wave 4 has been shifted back into the potential range of the solvent, suggesting that Cl^- is no longer bound to the Ru(II) dimers. The potential for this "new" wave 4 is approximately 50 mV anodic of the original potential observed in CH_3CN, 0.1 M

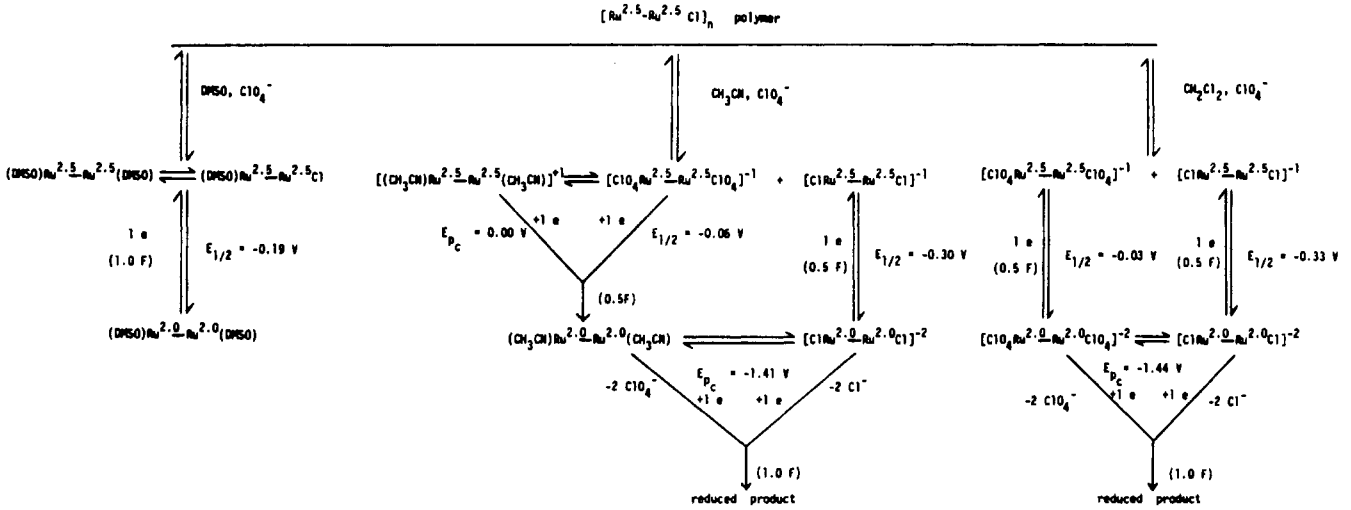

Figure 6. Reaction path for the electrochemical behavior of $Ru_2(HNOCCF_3)_4Cl$ in Me_2SO, CH_3CN, and CH_2Cl_2 solutions.

TBAP, and coincides with the shoulder of this wave, which we have attributed to an acetonitrile or ClO_4^- complexed species. In addition, the reversibility of this process appears to increase. This is shown in Figure 3d and suggests the replacement of Cl^- by a solvent molecule after AgCl precipitation. The fact that wave 2 remains (although it is slightly lower in current) suggests that, in the absence of a bound Cl^-, an equilibrium exists between two CH_3CN and ClO_4^- bound species.

On the basis of the cyclic voltammetric, titrimetric, and coulometric data, the overall reduction scheme shown in Figure 6 is postulated. In all solvents discrete dimeric units of Ru-($II^1/_2$) exist, but these species differ significantly in the type of axial ligation. The most simple reduction is in strongly bonding solvents such as Me_2SO. Only a single reduction process is observed, which consumes 1 faraday of electrons. On the basis of this result, the reaction is postulated to be

$$Ru(II^1/_2)\text{–}Ru(II^1/_2) + e^- \rightleftarrows Ru(II)\text{–}Ru(II) \quad (5)$$

Despite the observation of a single electrochemical process differently complexed Ru($II^1/_2$) dimers may be present in solution, as shown:

$$[(Me_2SO)Ru\text{–}Ru(Me_2SO)]^+ + Cl^- \rightleftarrows (Me_2SO)Ru\text{–}RuCl + Me_2SO \quad (6)$$

Since Cl^- is present at 10^{-3} M and Me_2SO is ~13 M, the equilibrium is shifted toward the left and the reaction at –0.19 V may be written

$$[(Me_2SO)Ru\text{–}Ru(Me_2SO)]^+ + e^- \rightleftarrows (Me_2SO)Ru\text{–}Ru(Me_2SO) \quad (7)$$

Electrochemical behavior similar to that observed in Me_2SO occurs in other strongly bonding solvents such as DMF, DMA, and CH_3OH (see Table I). The peak separation $|E_{p,a} - E_{p,c}|$ of the single process indicates that the redox couple is more irreversible in DMF and DMA than in Me_2SO. In contrast, reaction 5 is totally reversible in CH_3OH. One can envision $[(CH_3OH)Ru\text{–}Ru(CH_3OH)]^+$ as the reacting species which is easily reduced at –0.07 V. This potential is close to the value of 0.00 V measured for the first reduction in CH_3CN and suggests that this reaction is due to a bis-solvated species.

As already mentioned (and shown in Figure 2), four separate reductions of $Ru_2(HNOCCF_3)_4Cl$ are obtained in CH_3CN, 0.1 M TBAP. The first two of these reactions involve species in equilibrium and require a total 0.5 faraday for reduction of both complexes. The third process also requires 0.5 faraday for reduction but does not involve a species in rapid equilibrium with the first two. This was verified both by spectroscopic measurements of the reduction products (discussed in later sections) and by controlled-potential electrolysis at potentials between the two waves. After consumption of 0.5 faraday, the reaction appeared to stop and the currents for the second process did not decrease. This would suggest either a species not in equilibrium or a very slow equilibrium. On the basis of the potentials and titrations of $Ru_2(HNOC-CF_3)_4Cl$ with Cl^- and with Ag^+, the reactants may be considered to be an equilimolar mixture of the bis-dichloro dimer and another two species which are in equilibrium and which do not contain bound Cl^-. Because of the added negative charge on $[(Cl)Ru\text{–}Ru(Cl)]^-$, this species would be reduced at the more negative potential.

All of the reduction products appear to be dimers of Ru(II), but similar to the case for the starting mixture, these also differ in terms of their axial coordination. The product of $[(Cl)-Ru\text{–}Ru(Cl)]^-$ reduction is also a bis-dichloro species which is in equilibrium with one or more Ru(II) dimers not containing bound Cl^-. The potentials for further reduction of all forms of Ru(II) are very similar, and two overalpping processes are observed at approximately –1.41 V. These irreversible reactions consume 1 faraday of electrons, which is equal to the sum of the preceding three reactions.

Electronic Absorption Spectra of Ru($II^1/_2$) and Ru(II) Species. The UV–visible spectra of $Ru_2(HNOCCF_3)_4Cl$ in CH_2Cl_2, CH_3CN, and Me_2SO without supporting electrolyte are shown in Figure 7, and a summary of the maximum wavelengths and molar absorptivities is listed in Table III. In all three solvents a broad peak is present between 423 and 459 nm. In addition there is a shoulder at 463 nm in CH_2Cl_2 and 499 nm in CH_3CN. This smaller absorption, which is not observed in Me_2SO solutions, may be attributed to the presence of bound Cl^- ion and is due to a Cl^- to metal charge transfer which has been described in the literature.[16] Verification of the shoulder as being due to bound Cl^- was obtained by a spectral titration of $[Ru_2(HNOCCF_3)_4(Me_2SO)_2]^+$ with Cl^- in Me_2SO. As can be seen in Figure 8a, addition of 10^{-1} M Cl^- produced a spectrum similar to that seen in CH_3CN (Figure 7). Absorption maxima and molar absorptivities under these conditions are listed in Table III.

In CH_3CN a small peak was also observed at λ_{max} = 601 nm. This peak substantially increased upon addition of Ag^+ (Figure 9) to a solution of $Ru_2(HNOCCF_3)_4Cl$ in CH_3CN, 0.1 M TBAP, and may be attributed to a charge transfer involving either bound solvent molecules or bound ClO_4^-.

The spectra obtained during electrochemical reduction of $Ru_2(HNOCCF_3)_4Cl$ in Me_2SO are shown in Figure 10 with and without Cl^- ion. In Me_2SO solutions containing 0.1 M

Table III. Absorption Maxima and Molar Absorptivities of $Ru_2(HNOCCF_3)_4Cl$ and $Ru_2(HNOCCF_3)_4$ in CH_2Cl_2, CH_3CN, and Me_2SO Solution

solvent	supporting electrolyte	λ_{max}, nm ($10^{-3}\epsilon$)			
		$Ru_2(HNOCCF_3)_4Cl$			$Ru_2(HNOCCF_3)_4$
CH_2Cl_2	none	423 (0.29)	463 sh		546 (0.78)
	0.1 M TBAP	439 (0.35)	534 sh		554 (0.83)
CH_3CN	none	454 (0.72)	499 sh	601 (0.27)	628 (1.04)
	0.1 M TBAP	454 (0.72)	499 sh	601 (0.36)	630 (1.07)
	0.1 M (TBA)Cl	456 (0.81)	520 sh		
	0.1 M (TMA)Cl	456 (0.80)	520 sh		
Me_2SO	none	459 (0.61)			641 (1.31)
	0.1 M TBAP	459 (0.61)			641 (1.33)
	0.1 M (TBA)Cl	459 (0.66)	521 sh		
	0.1 M (TMA)Cl	459 (0.66)	521 sh		

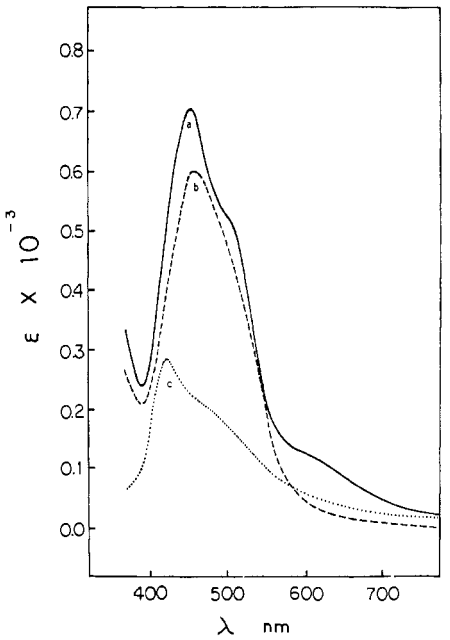

Figure 7. Electronic absorption spectra of $Ru_2(HNOCCF_3)_4Cl$ in (a) CH_3CN (—), (b) Me_2SO (---), and (c) CH_2Cl_2 (···). In this last solvent without TBAP the complex exists in a partially polymerized form.

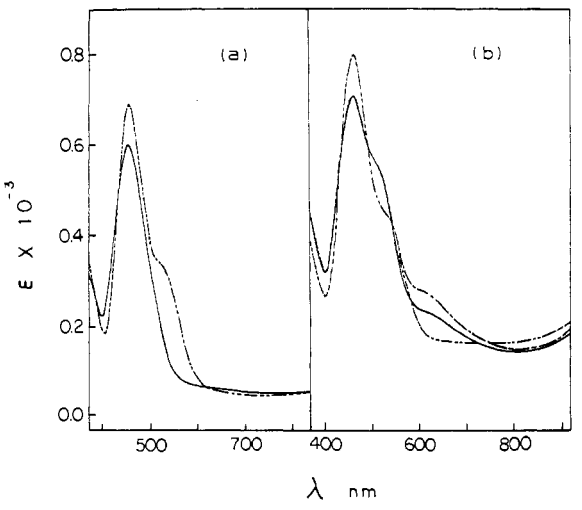

Figure 8. Electronic absorption spectra of $Ru_2(HNOCCF_3)_4Cl$: (a) in Me_2SO with (- - - - -) and without (—) added 0.1 M (TBA)Cl; (b) in CH_3CN without supporting electrolyte (—), with 0.1 M TBAP (- - -), and with 0.1 M (TBA)Cl (- - - - -).

TBAP there is a clear transformation of the $(Me_2SO)_2$ spectra to a new species having an absorption band at λ_{max} = 641 nm. This band is not present when the supporting electrolyte is 0.1 M (TBA)Cl (Figure 10b). With (TBA)Cl as supporting

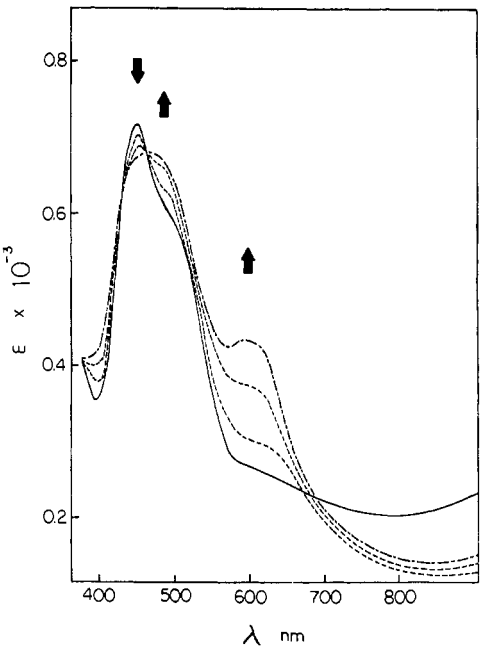

Figure 9. Electronic absorption spectra of $Ru_2(HNOCCF_3)_4Cl$ in CH_3CN at various mole ratios of $[Ag^+]/[Ru_2(HNOCCF_3)_4Cl]$: (1) 0.00 (—); (2) 0.20; (3) 0.50; (4) 1.00 (- - - -). Spectra 2 and 3 are given by the dashed lines.

electrolyte the Ru(II) product is most likely $[Ru_2(HNOCCF_3)_4(Cl)_2]^{2-}$ or $[Ru_2(HNOCCF_3)_4Cl(Me_2SO)]^-$ while with 0.1 M TBAP the reduction product is most likely $Ru_2(HNOCCF_3)_4(Me_2SO)_2$.

Spectra taken during stepwise controlled-potential electrolysis of $Ru_2(HNOCCF_3)_4Cl$ in CH_3CN, 0.1 M TBAP, are shown in Figure 11. Coulometric values for each step are shown in Table II. When the electrolysis was done at −0.2 V, the broad peak at 454 nm decreased and a new peak at 601 nm appeared (Figure 11a). Three isosbestic points were found at 424, 477, and 780 nm, as the solution changed from brown to blue. When the potential was set at −0.5 V, the peak at 454 nm totally disappeared and the peak at 601 nm further increased and shifted to 628 nm (Figure 11b). In addition, three isosbestic points were obtained at 425, 546, and 783 nm as the solution color turned a darker blue. Finally, Figure 11c illustrates the spectra of the green solution obtained after further electrolysis at −1.5 V. Again, there are isosbestic points indicating the presence of only two species in solution.

Electrochemistry of $Ru_2(O_2CC_3H_7)_4Cl$ in CH_3CN. The redox reactions of $Ru_2(O_2CC_3H_7)_4Cl$ (Figure 1a) have been reported in CH_2Cl_2, CH_3CN, and ethanol.[17] In CH_2Cl_2, 0.1 M TBAP, two reduction waves were observed which were approximately of equal height. Half-wave potentials were reported as 0.00 and −0.34 V. These potentials were independent of the electrode material (Pt, C, or Au) and were the

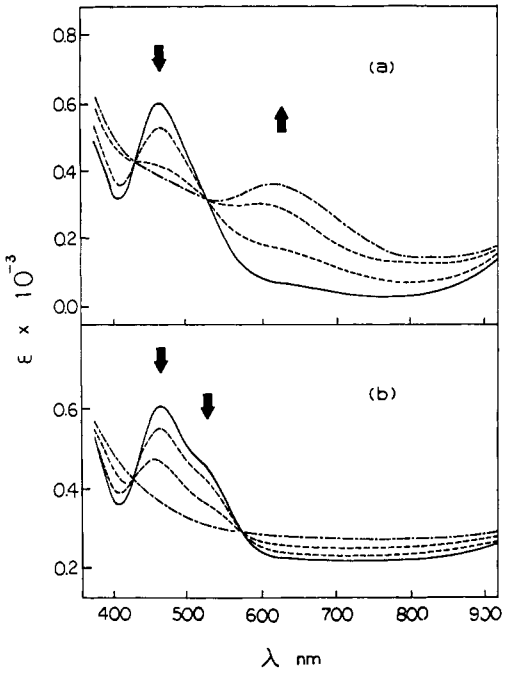

Figure 10. Time-resolved electronic absorption spectra of $Ru_2(HNOCCF_3)_4Cl$ obtained after reduction at −0.5 V in Me_2SO: (a) with 0.1 M TBAP; (b) with 0.1 M (TBA)Cl.

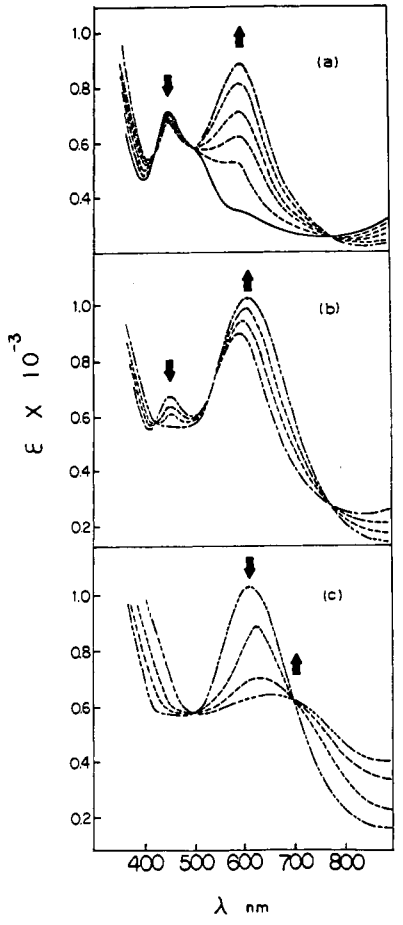

Figure 11. Time-resolved electron absorption spectra of $Ru_2(HNOCCF_3)_4Cl$ obtained in CH_3CN, 0.1 M TBAP, during controlled-potential reduction at (a) E_{app} = −0.2 V, (b) E_{app} = −0.5 V, and (c) E_{app} = −1.5 V.

only waves observed between −2.0 and +2.0 vs. SCE. Addition of Cl^- ion in the form of (TBA)Cl produced a decrease in the first reduction wave and an increase in the second such that,

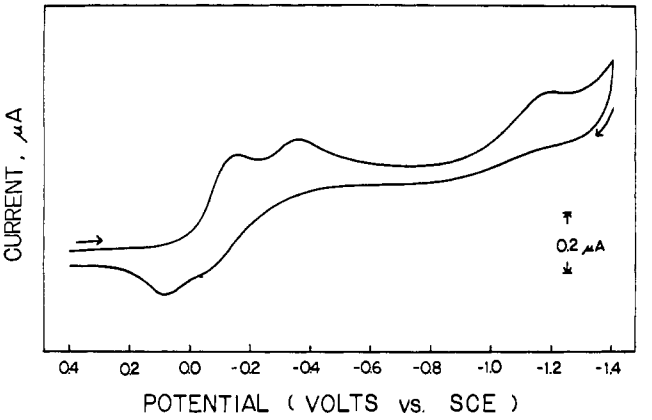

Figure 12. Cyclic voltammogram of $Ru_2(O_2CC_3H_7)_4Cl$ in CH_3CN, 0.1 M TBAP. Scan rate = 0.1 V/s.

Table IV. Half-Wave Potentials, Stepwise Coulometric Measurements, Absorption Maxima, and Molar Absorptivities of $Ru_2(O_2CC_3H_7)_4Cl$ in CH_3CN, 0.1 M TBAP, Solution

wave	$E_{1/2}$, V	e consumed, faraday	λ_{max}, nm ($10^{-3}\epsilon$)		
before electrolysis			458.3 (1.23)		
1	−0.05	0.63	458.3 (1.01)	564.4 (0.67)	
2	−0.28	0.38	...	572.9 (1.65)	
3	−1.20	0.95	...	580.2 (1.02)	651 sh

with 0.1 M (TBA)Cl, only one electrochemical process was observed.[17] A similar monotonic process was also reported in ethanol containing 0.1 M (TBA)Cl. Based on the current–voltage curves, the experiments with Cl^- addition, and the investigated ESR properties of $Ru_2(O_2CC_3H_7)_4Cl$, the reduction mechanism was analyzed as shown:

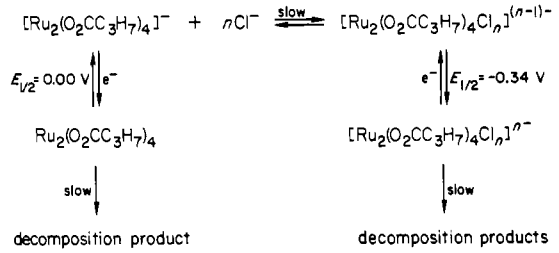

We have confirmed these experimental results in this study, although our results are somewhat at variance in CH_3CN, where a third irreversible wave is observed at negative potentials. This is shown in Figure 12. Controlled-potential reduction shows that 0.63 faraday is consumed in the first reduction ($E_{1/2}$ = −0.05 V) and 0.38 faraday in the second reduction ($E_{1/2}$ = −0.28 V). The third irreversible reduction (at $E_{p,c}$ = −1.20 V) consumes 0.95 faraday (Table IV).

Spectra generated during controlled-potential reduction are shown in Figure 13 and the wavelengths of the resultant products summarized in Table IV. During the first reduction, the peak at 458 nm for $Ru_2(O_2CC_3H_7)_4Cl$ decreases and a new band at 564 nm appears. There is a clear isosbestic point at λ = 496 nm indicating only two species in solution. Further reduction at potentials cathodic of wave 2 (−0.8 V) generate the species shown in Figure 13b. Again there is a clear isosbestic point indicating the presence of only two species in solution. Finally electrochemical reduction at a potential of −1.35 V produces a new species with a peak at 580 nm and a shoulder at 651 nm. Similar to the other reductions an isosbestic point is obtained. All of these spectra are similar to those observed during the controlled-potential reduction of $Ru_2(HNOCCF_3)_4Cl$ and closely resemble the products obtained in Me_2SO.

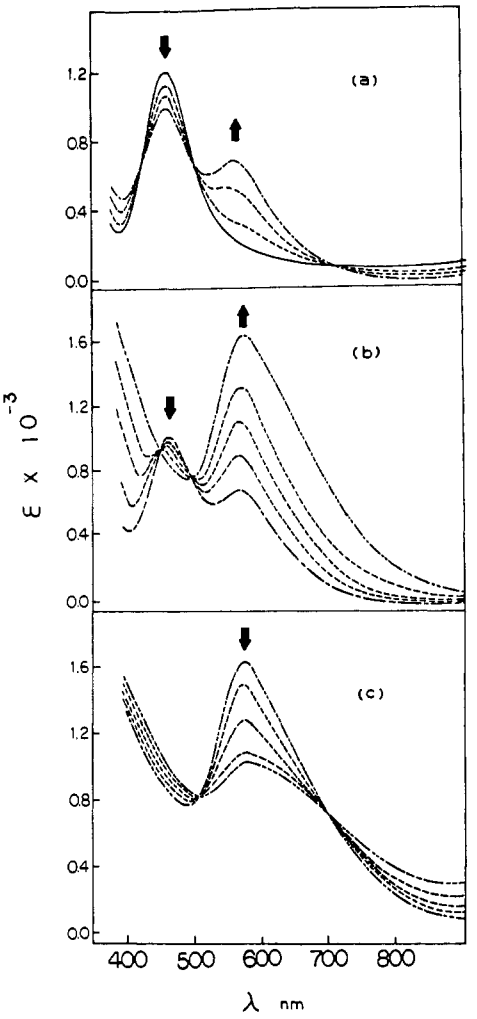

Figure 13. Time-resolved electron absorption spectra of $Ru_2(O_2CC_3H_7)_4Cl$ obtained during controlled-potential reduction in CH_3CN, 0.1 M TBAP (a) at $E_{app} = -0.2$ V, (b) at $E_{app} = -0.8$ V, and (c) at $E_{app} = -1.35$ V. The solid line in part (a) is the spectrum before reduction.

In order to have a direct comparison between $Ru_2(HNOCCF_3)_4Cl$ and $Ru_2(O_2CC_3H_7)_4Cl$ redox properties, the latter compound was electrochemically and spectrally investigated in three solvents containing 0.1 M TBAP and 0.1 M (TBA)Cl. The results of these studies are summarized in Table V. As seen in this table, both compounds undergo only one redox process in CH_3OH, 0.1 M TBAP, or CH_2Cl_2 and CH_3CN containing 0.1 M (TBA)Cl. With 0.1 M TBAP as supporting electrolyte in CH_2Cl_2 and CH_3CN, both compounds have two reductions that are also at virtually identical potentials. In contrast, however, the most negative reduction process in CH_2Cl_2 and CH_3CN differs by 140 to 210 mV between the two Ru(II) complexes. This difference in E_p might be attributed to differences in associated redox or chemical kinetics of the individual processes.[19] On the other hand, this anodic shift of potential for $Ru_2(O_2CC_3H_7)_4Cl$ could also be a result of the more weakly bonded Ru(II) dimer being more susceptible to the equatorial bonding environment. In other words, as the metal–metal bond becomes weaker due to decreasing bond order, the orbital pattern becomes more susceptible to bonding perturbations. In this case the less electronegative nitrogen would add more electron density to the

(19) Increased values of the electron transfer rate constant (k°) or the rate of an associated chemical reaction following electron transfer would produce an anodic shift of potential. The magnitude of this shift cannot be ascertained without an exact measurement of the rate constant.

Table V. Comparison of Potentials for $Ru_2(HNOCCF_3)_4Cl$ and $Ru_2(O_2CC_3H_7)_4Cl$ in CH_2Cl_2, CH_3CN, and CH_3OH (Scan Rate 0.1 V/s)

solvent	supporting electrolyte	$E_{1/2}$, V vs. SCE	
		$Ru_2(HNOCCF_3)_4Cl$	$Ru_2(O_2CC_3H_7)_4Cl$
CH_2Cl_2	0.1 M TBAP	−0.03	−0.02
		−0.33	−0.35
		(−1.44)[a]	(−1.30)[a]
	0.1 M (TBA)Cl	−0.26	−0.36
CH_3CN	0.1 M TBAP	(0.00)[a]	
		−0.06	−0.05
		−0.30	−0.28
		(−1.41)[a]	(−1.20)[a]
	0.1 M (TBA)Cl	−0.34	−0.36
CH_3OH	0.1 M TBAP	−0.07	−0.05

[a] Potential reported is $E_{p,c}$.

Ru(II) atoms, making a harder reduction.

It is worth noting that a small peak appears at 0.0 V in CH_3CN for $Ru_2(HNOCCF_3)_4Cl$ but not for $Ru_2(O_2CC_3H_7)_4Cl$. This peak (which is quite small) has been ascribed as due to formation of the bis-solvated species for the amidato complex and suggests that similar solvation is not present in the case of the carboxylato Ru(II) species. Because the currents are quite small for this wave, only a minor decrease in formation constant for the dichloro complex would result in its disappearance. Thus, no significance can be attributed to the absence of this peak in $Ru_2(O_2CC_3H_7)_4Cl$.

The above spectral data, as well as the similarity in the cyclic voltammetry of $Ru_2(HNOCCF_3)_4Cl$ and $Ru_2(O_2CC_3H_7)_4Cl$ (Table V), suggest that the actual reduction mechanism of the two compounds in CH_3CN, 0.1 M TBAP, are similar and can be described as shown in Figure 6. The mechanism also appears to be similar in Cl^- media and can be described by eq 4 and 8. The binding of two Cl^- ions to the Ru(II) dimer

$$[Ru_2(O_2CC_3H_7)_4Cl_2]^- + e^- \rightleftarrows [Ru_2(O_2CC_3H_7)_4Cl_2]^{2-} \quad (8)$$

is strongly suggested by the invariance of the wave with added Cl^- as observed in this study and suggested in an earlier one by Cotton and Pedersen.[17]

In conclusion, we have characterized the electrochemistry and spectroelectrochemistry of a novel $Ru(II^1/_2)$ amidato dimer and have compared these results to those obtained for reduction of a $Ru(II^1/_2)$ carboxylato dimer. In addition to obtaining new spectral data for reduced $Ru_2(HNOCCF_3)_4$ and $[Ru_2(HNOCCF_3)_4(Cl)_2]^{2-}$ complexes, we have also generated, for the first time, similar spectral data for $Ru_2(O_2CC_3H_7)_4$. It was previously reported that crystalline samples of $Ru_2(O_2CR)_4$ have never been obtained, although the species probably exists in solution.[8,10,17] Our study indicates that those species almost certainly exist in solution, often in the form $Ru_2(O_2CR)_4X_2$ or $Ru_2(HNOCR)_4X_2$, where X may be Cl^-, ClO_4^-, solvent, or various combinations of these.

Contrary to what one might have expected, $Ru_2(HNOCCF_3)_4Cl$, which is the first reported $Ru(II^1/_2)$ dimer with amidato bridging ligands, shows an electroreduction mechanism similar to that of one of the known ruthenium chloro carboxylates, $Ru_2(O_2CC_3H_7)_4Cl$. The magnetic moments and ESR spectrum obtained for $Ru_2(HNOCCF_3)_4Cl$ show that this new compound, like the ruthenium chloro carboxylates, has three unpaired electrons which are fully delocalized.[4,5,17] Although the potentials are virtually identical for reduction of these two complexes, it must be noted that a clear difference does exist in the type of electron-donating group attached to the bridging ligand. It has been shown for the case of $Rh_2(O_2CR)_4$ and $[Rh_2(O_2CR)_4]^+$ complexes that the substitution of a CF_3 group for C_3H_7 results in an anodic shift of over 600 mV in the reduction or oxidation potentials.[1] Thus, assuming the same linear free energy relationships, one could expect that

$Ru_2(O_2CCF_3)_4Cl$ would be initially reduced at close to +0.6 V, generating an extremely stable Ru(II) dimer.

Acknowledgment. Support of this research from the Robert A. Welch Foundation (K.M.K., Grant E-680; J.L.B., Grant E-196) is gratefully acknowledged. We also wish to thank Josianne Ginestra for the solid-state magnetic moment data.

Registry No. $Ru_2(HNOCCF_3)_4Cl$, 86846-89-1; $[Ru_2(HNOCCF_3)_4(Cl)_2]^-$, 86846-90-4; $Ru_2(O_2CC_3H_7)_4Cl$, 86846-91-5; $Ru_2(O_2CC_3H_7)_4$, 86846-92-6; $Ru_2(HNOCCF_3)_4$, 86846-93-7; $Ru_2(O_2CCH_3)_4Cl$, 38833-34-0; Ru, 7440-18-8; TBAP, 1923-70-2; (TBA)Cl, 1112-67-0.

Contribution from the Laboratoire d'Electrochimie et de Chimie Physique du Corps Solide, ERA au CNRS No. 468, Universite Louis Pasteur, 67000 Strasbourg, France

Electrochemical Reduction of Uranium(IV) Acetylacetonate in Aprotic Media

E. GRAF, A. GIRAUDEAU, and M. GROSS*

Received February 2, 1983

The electrochemical reduction of $U^{IV}(acac)_4$ has been investigated in propylene carbonate and acetonitrile solvents on mercury electrodes. The overall monoelectronic reduction of $U^{IV}(acac)_4$ to $[U^{III}(acac)_4]^-$ occurs in two distinct steps. Electrochemical measurements associated with temperature and/or drop-time changes show the presence of an intermediate chemical reaction following the first electrochemical step. Addition of basic molecules clearly demonstrates that the intermediate chemical step corresponds to the intermolecular exchange of one acac ligand between the oxidized and reduced forms of the acetylacetonate uranium complex, leading to the formation of the $[U^{IV}(acac)_5]^-$ complex. An interpretation resting on the nonoccupied ninth coordination position of uranium is given for this behavior.

Introduction

Redox properties of uranium in aqueous solutions have been studied by many investigators.[1-5] In aqueous media, hexavalent uranium UO_2^{2+} is reduced in two[1-3] or three steps,[4] depending on the pH and the nature of the supporting electrolyte. On the time scale of polarographic methods, the reduction of UO_2^{2+} occurs in three steps: the first is a reversible one-electron step resulting in the formation of quinquevalent uranium UO_2^+; this is followed by a second wave corresponding to the irreversible reduction of uranium(V) to uranium(IV); the third step corresponds to the reversible reduction of U^{IV} to U^{III}.[4] Direct reduction of U^V to U^{III} was also observed.[3,5]

On the other hand, electrochemical studies on U^{IV} solutions have shown that the system U^{IV}/U^{III} is reversible, with a half-wave potential close to that of the third polarographic wave of uranyl ion,[6] but it was noticed that the generated U^{III} species undergo fast chemical oxidation, probably due to the reduction of protons by U^{III}.

Such a chemical reduction of protons by electrochemically generated species may be prevented and, consequently, low oxidation states of uranium may be stabilized in solution, when appropriate organic solvents are used in electrochemical investigations.

In organic solvents the electrochemical reduction of U^{VI} and U^{IV} species to trivalent uranium has been previously reported[6-9a] but generally without mechanistic details. Also, obtention of zerovalent amalgamated uranium is not unambiguously established.[9b]

The present paper provides the first report of a study devoted to the redox behavior of tetrakis(acetylacetonato)uranium(IV) ($U^{IV}(acac)_4$). Previous studies on the reduction of acetylacetonates of several transition metals[10-12] have revealed that these reductions may trigger significant changes in the coordination of the metals and also that the coordinating acac ligands alter the redox reactivity of the central metal, and this is actually the basis of the current study.

Table I. Half-Wave Potentials of $U^{IV}(acac)_4$ (V/SCE at 20 °C) at a Dropping-Mercury Electrode[a]

	$E_{1/2}{}^1$	$E_{1/2}{}^2$
PC/TEAP	−0.780	−1.180
PC/TBAP	−0.800	−1.200
CH_3CN/TEAP	−0.780	−1.200
CH_3CN/TBAP	−0.780	−1.160

[a] Drop time 2 s; scan rate 2 $mV \cdot s^{-1}$.

X-ray data in the solid state and several consistent arguments[13] indicate that tetrakis(acetylacetonato)uranium(IV) has the D_2 square antiprism as the ground-state coordination polyhedron. In solution, ^1H NMR indicates a less symmetrical structure, and the experimental observations can be rationalized only by assuming two (or more) nonequivalent sites for this 8-coordinated chelate.

Also, it is generally accepted that the ring-shaped β-diketone ligand is a conjugated system, and it is demonstrated that unpaired spin density is transferred from the paramagnetic transition metal to the ligand, in β-diketonates of uranium(IV).[14]

In this work, the redox behavior of $U^{IV}(acac)_4$ will be discussed and a reduction mechanism will be proposed.

Experimental Section

The studied compound $U^{IV}(acac)_4$ was purchased from Pfaltz and Bauer, Inc. $[N(CH_3)_4]$acac salts were prepared according to known procedures.[15] Sodium methanolate was a commercial product (Merck).

Electrochemical measurements were carried out under argon at controlled temperatures (20 or −25 °C) on dropping-mercury electrodes. All measurements were performed with a classical three-

(1) Herasymenko, P. *Trans. Faraday Soc.* **1928**, *24*, 267.
(2) Kritchevsky, E. S.; Hindmann, J. C. *J. Am. Chem. Soc.* **1949**, *71*, 2096.
(3) Stabrowskii, A. I. *Zh. Neorg. Khim.* **1966**, *11*, 76.
(4) (a) Kanevskii, E. A.; Pavlovskaya, G. R. *Zh. Neorg. Khim.* **1960**, *5*, 1738. (b) *Ibid.* **1960**, *5*, 1965.
(5) Harris, W. E.; Kolthoff, I. M. *J. Am. Chem. Soc.* **1945**, *67*, 1484.
(6) Sipos, L.; Jeftic, L. J.; Branica, M.; Galus, Z. *J. Electroanal. Chem. Interfacial Electrochem.* **1971**, *32*, 35.
(7) Finke, R. G.; Hirose, Y.; Gaughan, G. *Chem. Commun.* **1981**, 232.
(8) Billiau, F.; Folcher, G.; Marquet-Ellis, H.; Rigny, P.; Saito, E. *J. Am. Chem. Soc.* **1981**, *103*, 5603.
(9) (a) Fedoseev, A. M.; Peretrukhin, V. F. *Radiokhimiya* **1979**, *21*, 650. (b) *Ibid.* **1979**, *21*, 655.
(10) Beaver, B. D.; Hall, L. C.; Lukehart, C. M.; Preston, L. D. *Inorg. Chim. Acta* **1981**, *47*, 25.
(11) Sock, O.; Lemoine, P.; Gross, M. *Electrochim. Acta* **1981**, *26*, 99.
(12) Dessy, R. E.; Stary, F. E.; King, R. B.; Waldrop, M. *J. Am. Chem. Soc.* **1966**, *88*, 471.
(13) Siddall, T. H.; Stewart, W. E. *J. Chem. Soc. D* **1969**, 922.
(14) Wiedenheft, C. *Inorg. Chem.* **1969**, *8*, 1174.
(15) Burnett, J. N.; Hiller, L. K., Jr.; Murray, R. W. *J. Electrochem. Soc.* **1970**, *117*, 1028.

0020-1669/83/1322-3233$01.50/0